Revista Mexicana de Astronomía y Astrofísica, **41**, 121–129 (2005)

DETERMINATION OF THE MASS LOSS RATE AND THE TERMINAL VELOCITY OF STELLAR WINDS. I. GENETIC ALGORITHM FOR AUTOMATIC LINE PROFILE FITTING

L. Georgiev and X. Hernández

Instituto de Astronomía
Universidad Nacional Autónoma de México

Received 2004 July 20; accepted 2005 January 27

RESUMEN

Se presenta un nuevo método de ajuste automático de perfiles P Cyg observados en espectros *UV* de vientos estelares. La función fuente de las líneas se calcula usando la aproximación de Sobolev y el flujo emitido se obtiene a través de la solución exacta de la ecuación de transporte (similar al método SEI descrito por Lamer et al. 1987). La calidad del ajuste se evalúa usando el estimador de verosimilitud. La maximización de la verosimilitud se hace a través de un algoritmo genético. Las ventajas de nuestro método comparado con otros métodos similares son su estabilidad y su poca sensibilidad de las condiciones iniciales. Además, el método garantiza la localización del máximo global de la superficie de verosimilitud, lo que no se puede hacer con los algoritmos clásicos. Presentamos la implementación del método, las pruebas de su funcionalidad usando datos sintéticos y reales y la estimación de los intervalos de confianza de los resultados.

ABSTRACT

A new method for automatic fitting of P Cyg line profiles in *UV* spectra of stellar winds is presented. The line source function is calculated using Sobolev's approximation and the emergent flux is obtained by exact integration of the equation of the radiation transport (similar to the SEI method described by Lamers et al. (1987)). The quality of the fit is evaluated using the likelihood estimator. The maximization of the likelihood is done by a genetic algorithm. The advantages of our method with respect to other similar approaches are its robustness and its insensibility to the initial guess. In addition, the algorithm guarantees the localization of the global maximum of the likelihood hypersurface, which is not the case for classical minimization algorithms. Here we present an implementation of the genetic algorithm for line profile fitting, its tests on both synthetic and real data and an estimation of the confidence limits of the results.

Key Words: **LINE: PROFILES — STARS: ATMOSPHERES — STARS: WINDS, OUTFLOWS**

1. INTRODUCTION

Many hot stars lose mass through a supersonic wind. The terminal velocity of these winds, and the details of the mass loss rate play an important role in stellar evolution. Stellar winds crucially determine the interaction of the star with its surrounding interstellar medium, this being one of the central feedback mechanisms which in turn modulate star formation at galactic levels. Estimating stellar mass loss rates is therefore a highly relevant problem.

The best way of determining the mass loss rate of a star is by studying the radio emission from the wind itself (Lamers et al. 1999). However, with current observational techniques this is limited to nearby stars with high mass loss rates. The other reliable method is based on a detailed modeling of the stellar spectrum. The recent development of realistic codes which include many atomic lines makes the latter approach the preferred one. Unfortunately, the fitting of the spectrum requires high quality data

covering a wide range of wavelengths and with high dispersion; this again limits the method to bright or nearby stars. An alternative has been proposed by Lamers, Cerruti-Sola, & Perinotto (1987) and Groenewegen & Lamers (1989). This method is based on a code which approximates the opacity of the wind as a simple function of the distance from the stellar nucleus. The code calculates the source function in a given line within the Sobolev approximation (Sobolev 1958) and then calculates accurately the emitted profile. The fit of the observed profile gives the terminal velocity of the wind together with the total optical depth along the line of sight. The mass loss rate is estimated from the latter (see next section). Even though the obtained value is sensitive to certain assumptions regarding the ionization fraction of the element whose line is fitted, the method has the advantage of being applicable to faint stars for which only low resolution and low signal to noise spectra are available.

The main disadvantage of this approach is the large number of free parameters which have to be adjusted. Groenewegen & Lamers (1989) proposed a method for determination of the parameters by a "classical" minimization of the $\chi^2 = \sum (1 - F_o/F_c)$ where F_o is the observed flux and F_c is the calculated one. But the multi-dimensional fitting converges to the correct solution only if the initial guess is close to the χ^2 minimum. The complex topology associated with the high-dimensional hypersurface being treated leads to the appearance of numerous local minima. The "classical" minimization methods usually get trapped in the local minimum close to the initial guess and miss the global one. The somewhat lengthy numerical procedure involved, again together with the large number of dimension of the problem, makes a dense sampling of the parameter space completely impractical. Recent years have seen the development of non-standard maximization techniques such as simulated annealing and genetic algorithms, particularly in connection with astrophysical applications (e.g., Teriaca, Banerjee, & Doyle 1999 fit radiative transfer models to solar atmosphere data; Sevenster et al. 1999 fit parameters of Galactic structure models to observations; Metcalfe 2003 fit white dwarf astroseismology parmeters). These methods provide a framework which in a reliable manner identifies the global maxima (or minima, as the case might be) of complex multi-dimensional surfaces, with a close to optimal use of computing resources.

In this paper we present an application of a genetic algorithm used to obtain the optimal parameters of a stellar wind, within the Sobolev approximation, for the fitting of P Cyg line profiles of *UV* resonance lines.

Section 2 describes the radiative transfer model. In §3 a description of the genetic algorithm is given, with use of it in a number of synthetic test cases and real data examples appearing in §4. Section 5 presents our conclusions.

2. THE ALGORITHM

2.1. *Radiative Transfer Code*

The core of the method is a code which solves the radiative transport problem under the assumption of a spherically symmetric stellar wind. Following the SEI code (Lamers et al. 1987) we approximate the radial Sobolev optical depth $\tau(v)$ as:

$$\tau(v) = \frac{\chi_0 c}{\nu_0 (dv/dr)} = T\, v^{\alpha_1} (1 - v)^{\alpha_2}\,, \qquad (1)$$

where $v = V(r)/V_\infty$ is the velocity of the wind, normalized to the terminal velocity V_∞, χ_0 is the central opacity of the line, ν_0 is the laboratory frequency of the transition and c is the speed of light. T, α_1, and α_2 are free parameters of the model, which describe the radial dependence of the optical depth. The velocity field of the wind is adopted to be a standard β-law

$$V(r) = V_\infty \left(1 - \frac{R_0}{r}\right)^\beta\,, \qquad (2)$$

where V_∞ is the terminal velocity. The winds of the hot stars are not smooth but have random motions. The shape of the blue wing of the P Cyg absorption component suggests that the intrinsic line profile has a width on the order of hundreds of kilometers per second. The physical nature of these random motions is not clear but they act as an additional line broadening mechanism similar to turbulence and are frequently called "turbulence" although they may have little to do with it. We model this chaotic motions assuming the intrinsic line profile to be Gaussian, defined as

$$\phi(v) = \frac{1}{\sqrt{\pi} V_{turb}} \exp[-(v/V_{turb})^2]\,. \qquad (3)$$

The turbulent velocity, V_{turb}, can be variable throughout the wind, but because its physical nature is not clear there is no model of its possible variability. To keep the model as simple as possible, we assume V_{turb} to be constant and a parameter of the model.

Finally, we set the innermost point of the grid, R_{min} to the location where $V(R_{min})$ is equal to the

sound speed V_{sound}. This is done by setting the parameter R_0 in Eq. (2) as:

$$R_0 = R_{min}\left[1.0 - \left(\frac{V_{sound}}{V_\infty}\right)^{\frac{1}{\beta}}\right]. \quad (4)$$

Equations (1), (2), and (4) determine the distribution of the central opacity of the line χ_0 as a function of the radius r. Within the Sobolev approximation one can now calculate the line source function S and can then apply a formal solution of the equation of radiative transport throughout the wind and calculate the emergent flux (see Georgiev & Koenigsberger 2004 for more details of the code). The code is designed to work in 3D geometry, but for the current test purposes the solution is restricted to the case of spherical symmetry. Finally, we calculate the mass loss rate as follows (Groenewegen & Lamers 1989). The line opacity χ_0 is

$$\chi_0 = \frac{\pi e^2}{mc} f_{lu} n_l = \tau(v) * \frac{\nu_0}{c}\frac{dV(r)}{dr}, \quad (5)$$

where n_l is the population of the lower level, f_{lu} is the oscillator strength and we do not take into account the correction for stimulated emission. The level population n_l can be written as:

$$n_l = N_{ion} q_{ex} = N_{atom} q_{ion} q_{ex} = N_H A_E q_{ion} q_{ex}, \quad (6)$$

where q_{ion} and q_{ex} are the ionization and excitation fractions and A_E is the chemical composition of the element relative to hydrogen by number. Then the level population n_l is related to the mass loss rate by the equation of continuity

$$n_l = \frac{A_E}{\mu}\frac{\dot{M} q_{ion} q_{ex}}{4\pi r^2 V(r)}, \quad (7)$$

where μ is the average molecular weight. Substituting (7) into (5), one can obtain the product $\dot{M} q_{ion} q_{ex}$ at each point r as:

$$\dot{M} q_{ion} q_{ex} = \tau(v)\frac{dV(r)}{dr} r^2 V(r)\frac{\mu}{A_E}\frac{4mc}{e^2 f_{lu}}\frac{\nu_0}{c}. \quad (8)$$

Then, if the parameters $V_\infty, V_{turb}, \beta, T, \alpha_1$ and α_2 are given, Eq. (1) and (2) together with the atomic data and the chemical composition allow the estimation of the product $\dot{M} q_{ion} q_{ex}$. The method described in this paper suggests a better way to obtain the six parameters that describe the velocity law and the optical depth. It may not improve the precision of the calculated mass loss rate if the dominant uncertainty is the ionization fraction.

Applying the above procedure we are able to calculate any line profile, once the six parameters of the method $V_\infty, V_{turb}, \beta, T, \alpha_1$, and α_2 have been specified. The next step is the selection of a statistical estimator of the goodness of fit to be associated to a particular set of parameters and a given observed profile. From a Bayesian perspective, the optimal such indicator is the likelihood, calculated as the probability that a certain data set be observed, given a model. We hence compare a modeled profile against a given observation through a likelihood estimator defined as:

$$\log L(V_\infty, V_{turb}, \beta, T, \alpha_1, \alpha_2) =$$
$$\sum_i \log\left[\frac{1}{(2\pi)^{1/2}\sigma_i} exp - \left(\frac{F_{i,o} - F_{i,c}}{2\sigma_i}\right)^2\right], \quad (9)$$

where $F_{i,o}$ and $F_{i,c}$ are the observed and calculated flux respectively at a certain wavelength, λ_i and the factors σ_i are the observational errors at the same λ_i. The weight σ assigned to each observed point is taken from the signal-to-noise ratio of the observations. Setting a large σ_i to certain points forces them to participate less in the final fit, which allows us to exclude effectively spectral regions where overlap with other lines occurs. Hence, the final result depends on the assigned σ_i. In practice, the bands of the observed spectrum affected by spurious details are easily detectable and the assignment of the weights is straightforward.

The synthetic profile is calculated over a grid adjusted for better sampling the velocity field in the wind. The calculated profile is then interpolated on the wavelengths of the observed profile using monotonic cubic polynomials (Steffen 1990). Finally, Eq. (9) is calculated and used as a measure of the quality of the fit.

2.2. *The Genetic Algorithm*

Once we have a method for calculating the line profile which corresponds to a particular set of six parameters, and an estimator of the goodness of the fit, we must now determine what the optimal parameter vector is; i.e., we must find the combination of six parameters which maximizes our likelihood function. This will yield the physical parameters of the stellar wind associated to the observed line profile, from which the mass loss rates and wind terminal velocities can be estimated.

A dense exploration of our six-dimensional parameter space is unfeasible. Classical maximization techniques are also unreliable in connection to problems of such high dimensionality, and liable to get

trapped by local maxima. In fact we have encountered numerous test cases where local maxima exist in the likelihood surface of our problem. We bypass these obstacles using genetic algorithms in searching for the maximum of the likelihood surface.

The idea is to simulate a population of organisms (we call them "bugs") which breed and evolve following prescriptions based on those biological systems are thought to follow, the result being a progressive increase in the fitness of the population, with the fittest individual in each generation eventually reaching the absolute maximum of the fitness surface. For the case at hand, a "bug" is a set of wind parameters described above.

Once an observed line profile has been picked, the first step is to select N random points in our parameter space, each a parameter vector for the stellar wind, $(V_\infty, V_{turb}, \beta, T, \alpha_1, \alpha_2)$. The ranges over which these parameters are to be chosen have to be determined by inspection of the observed line profile. Only ample margins enclosing the expected value are needed. We turn to this issue in the examples section.

The six coordinates of each point are turned into binary numbers, with a pre-determined resolution and then combined in a string. We have used 8 bits per parameter for our implementation, resulting in a string of $N_G = 6$ parameters $\times 8$ bits $= 48$ bits. This selection gives to our search algorithm a resolution of $Range_i/2^8$ in each of the six dimensions where $Range_{1-6}$ are the ranges for each parameter chosen above.

Each of the N randomly selected points becomes a "bug" of the first generation. The string of N_G 1^s and 0^s which corresponds to its 6 coordinates in parameter space becomes its "genotype", and the likelihood associated to that point becomes its "phenotype". The N members of the first generation are then ranked according to the value of the likelihood associated to each, with those ranking above N/S_P being deemed "superior", and those ranking below this threshold "inferior". S_P is a parameter of the simulation which has to be a number greater than 1.0, typically around 1.5.

This completes the first generation, which are now "mated" to produce the second one. This proceeds by the random selection of pairs of individuals from the pool of N members of the first generation. Once a pair is selected, "offspring" are calculated. The first C_P genes of one of the parents are taken for first C_P genes of the offspring, and the remainder are taken from the other parent. C_P is a "crossing point", chosen at random in the interval (0-N_G), each time an offspring is constructed.

In this way, the offspring will have "genes" in some aspects resembling those of one parent, and in some cases the other, the corresponding position in parameter space will hence share some coordinates with one parent, and some with the other, with one of them being a mixture. Also, a fraction M_F of randomly selected genes in the new generation are "mutated" i.e., they are flipped from 1 to 0, or 0 to 1, as the case might be. M_F is a second and last parameter of the method, which together with S_P must be chosen and tuned through some testing of the algorithm in the context of the particular problem being treated. We have used M_F close to 0.01 which means that 1% of the genes are mutated.

The number of offspring to be produced by each pair depends on the fitness of the parents; if both are "superior" individuals, 3 offspring are calculated. The pairing of a "superior" and an "inferior" individual yields only 2 offspring, and when two unfortunate "inferiors" mate, only one child ensues. The process is repeated until N offspring have been obtained, the new generation has been constructed, and it completely replaces the former.

The parameter S_P hence represents a selection pressure. If chosen close to 1, most individuals will be deemed "superior", and hence the second generation will be distributed in parameter space much like the first one was. However, as S_P takes larger values, the second generation will be made up of the sons of (mostly) the "superior" individuals of the former, yielding a gradual climb up the likelihood surface of the problem. Next, the genotypes of the new generation are turned back into coordinates in our parameter space, and then into phenotypes — the associated likelihood. The ranking is repeated, and the cycle iterated.

In this way, we have introduced mating, selection, and chance mutations, the three main ingredients of biological evolution, albeit in a highly simplified manner. Selection forces subsequent generations up the likelihood surface, with the random mutations ensuring that a fraction of the individuals are constantly sampling new regions, which in turn guarantees that the absolute maximum will eventually be found.

In many classical maximization algorithms one is called to evaluate the gradient of the surface at any given point. When the surface is not an analytical one, but the result of a lengthy numerical procedure, as in our case, the gradients could quite easily be dominated by roundoff errors. The method described calls for no gradients of the surface, only its

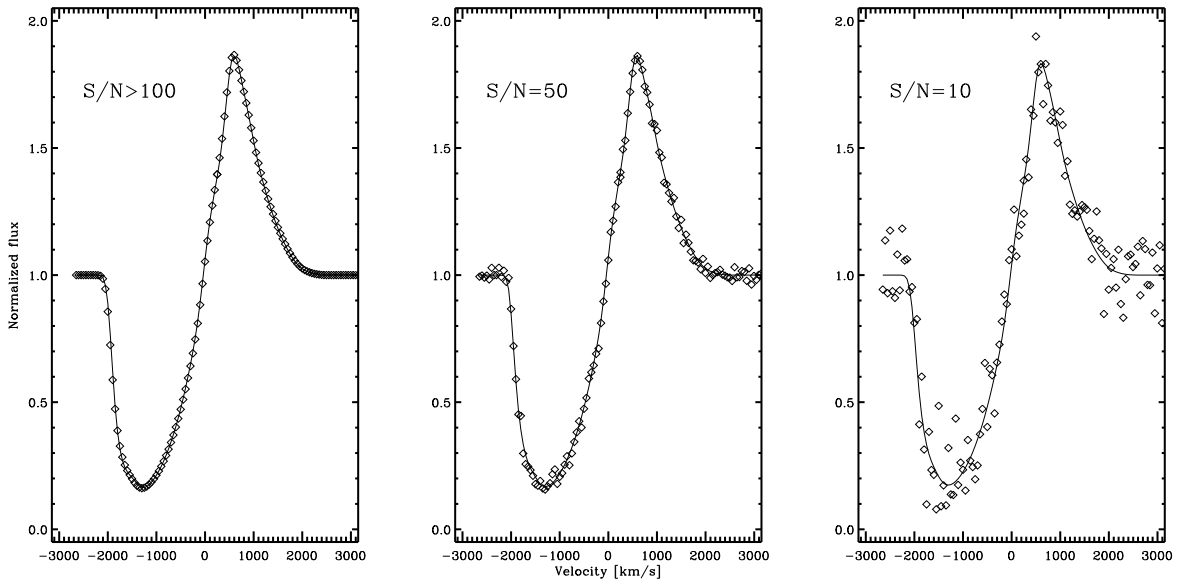

Fig. 1. Test of the fitting algorithm. A synthetic profile of C IV 1548/1550Å (squares) is shown together with the best fit (solid line) for three adopted S/N ratios.

value at the points being tested. With the resolution described here, a dense sampling of our likelihood surface would have required $(2^8)^6 = 2.8 \times 10^{14}$ evaluations of our wind model. We have used N = 100 members per generation, and both in synthetic examples where the answer was known in advance, and in tests with real data, have found convergence in 200 generations, i.e., only 2×10^4 costly line profile calculations.

The method described here differs only slightly from the general purpose genetic maximization algorithm PIKAIA, described in Charbonneau (1995), and having been used successfully in a number of astrophysical applications to date (e.g., Teriaca et al. 1999; Metcalfe 2003). The differences between the two are limited to the way "selection" is treated, the implementation described here giving results more suitable for the particular problem we are treating.

3. TEST CASES

The first test of the algorithm is made on synthetic data. We calculate the line profile of the C IV 1548/1550Å doublet with a predefined velocity law and wind density distribution and then fit this profile using the genetic algorithm. Figure 1 shows the original profile and the resulting fit for three different signal-to-noise ratios. The parameters used to generate the profile and the result of the fitting are summarized in Table 1.

The genetic algorithms do not include an easy way of estimating the errors of the results. The method only serves to locate the global maximum in an efficient manner. We estimate the confidence intervals of the recovered parameters by Monte-Carlo simulations of synthetic line profiles. In this way, all uncertainties inherent to the method and the modelled data are taken into account. We select three signal-to-noise ratios: 100, 50, and 10. For each of them we generate 20 different line profiles, using the same synthetic data but adding different and independent noise. The obtained line profiles were fitted by the genetic algorithm using different first generations of "bugs". Figures 2, 3, and 4 show the confidence intervals obtained through this method for the recovered parameters for the simulated profiles of Fig. 1.

Once the Monte-Carlo simulations are all done, we find the means for all the recovered parameters, and of the recovered mass loss rates. Next, a full covariance analysis is performed, yielding the parameters' standard deviations, which together with the relevant covariances can be used to construct statistically meaningful confidence ellipses. Fig. 2 shows the 1σ ellipses for the case of S/N =100, with the solid dots indicating the input values, and the circles showing the ones reached by the fitting algorithm. The mass loss rate is recovered almost exactly, with a 1σ interval of 30%. A negative correlation is seen between the inferred $\dot{M}$ and the recovered terminal wind velocity, while mass loss rate and β show a weak positive correlation. Figs. 3 and 4 are equivalent to

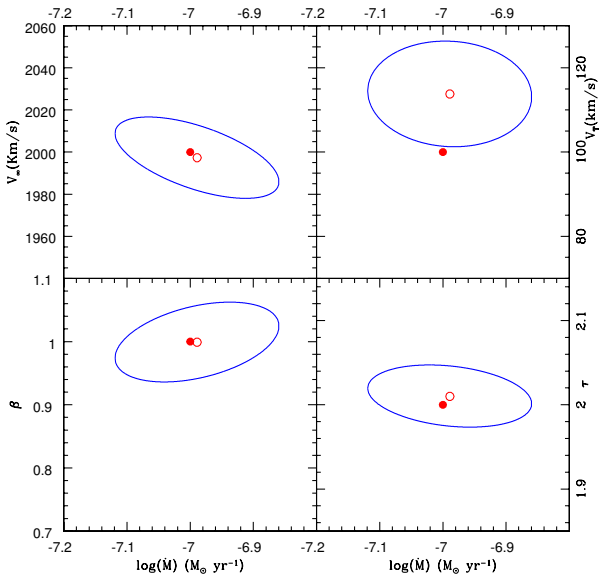

Fig. 2. The ellipses show 1σ confidence intervals on the recovered parameters (circles) for the fit to the synthetic profile with S/N = 100. The input values are shown by solid dots.

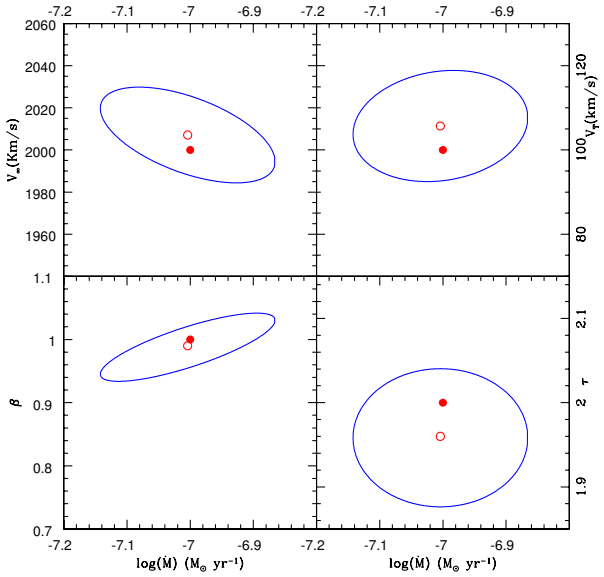

Fig. 3. The ellipses show 1σ confidence intervals on the recovered parameters (circles) for the fit to the synthetic profile with S/N = 50. The input values are shown by solid dots.

Fig. 2, but for the cases with S/N values of 50 and 10, respectively. The same qualitative features can be seen, with the ellipses getting only slightly larger, to reach 40% for the S/N = 10 case. It is reassuring that errors of the inferred mass loss rate are not highly sensitive to the value of the S/N of the simulated profile, making the method useful even in cases where observations are not of the best quality. Also, we note that no systematics appear on the recovered $\dot{M}$; we have constructed an unbiased estimator of the important physical parameter we set out to infer. We have to stress that the errors in the mass loss rate are the formal errors of the fit. The errors related to the determination of the ionization fraction will be treated in the next paper of the series.

As can be seen from Table 1 in all cases the algorithm finds the correct maximum of the likelihood estimator, the mass loss rate is recovered successfully, always well within 1σ of the input value, even at low S/N values. As an additional check we tried to fit the line profiles of real stars. Figure 5 shows the profile of the C IV 1548/1550 Å doublet observed in the IUE spectrum of ζ Pup (HD 66811) and Figure 7 shows the profile of the Si IV 1398/1402 Å doublet in the IUE spectrum of HD 30614. The comparison between the results of our fit and the parameters obtained by Groenewegen & Lamers (1989) (Table 2) shows a good agreement. Our solution shows a slower velocity law (large β) but our final fit has higher likelihood than the fit obtained with the published parametes. For both stars we obtain a larger V_∞ and lower V_{turb}. As shown in Figure 6, the two parameters are correlated and one could expect this behavior. But in both cases the automatic fit gives

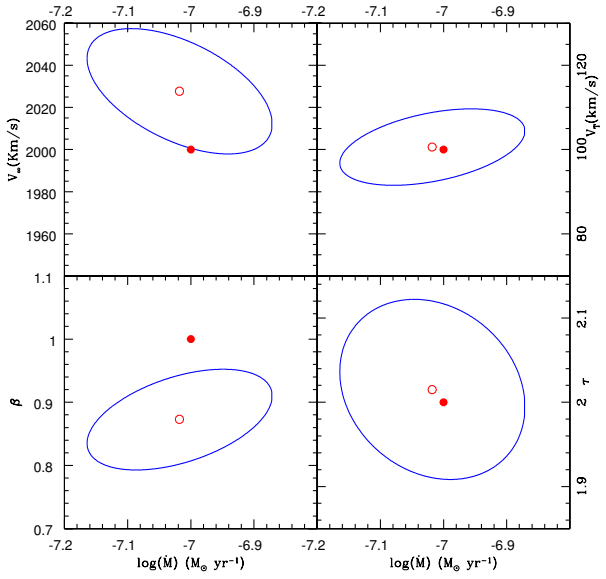

Fig. 4. The ellipses show 1σ confidence intervals on the recovered parameters (circles) for the fit to the synthetic profile with S/N = 10. The input values are shown by solid dots.

TABLE 1

PARAMETERS OF THE SYNTHETIC PROFILE AND THE RESULTS OF THE FITS

Parameter	Exact Value	S/N = 100	S/N = 50	S/N = 10
V_∞ (km s^{-1})	2000	1997±19	2007±23	2014±30
V_{turb} (km s^{-1})	100	114±12	107±13m	101±9
β	1.0	0.99±0.06	0.99±0.05	0.87±0.08
T	2.0	2.01±0.06	1.96±0.08	2.015±0.11
$\log \dot{M} q_{ion} q_{ex}$ ($M_\odot$/yr)	−7.0	−7.00±0.13	−7.00±0.14	−7.02±0.15

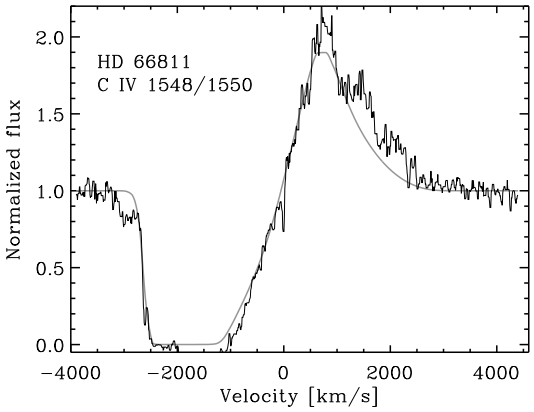

Fig. 5. Fit of the C IV 1548/1550 Å line in ζ Pup (=HD 66811). The thin line is the observed spectrum. The dotted line is the fit.

values very close to the more human-controlled solution.

4. CONCLUSIONS AND DISCUSSION

The determination of the basic stellar parameters like wind velocity and mass loss rate is a very time-consuming process. In this paper we present a method which allows an objective determination of these parameters based on a completely automatic procedure. The test cases shown above support the robustness of the method even in case of low S/N data. The method is especially useful for objects for which only low resolution and low S/N data are available. Their spectra show only few spectral features and the application of full NLTE codes is not practical. Our method was successfully applied by Arrieta & Stangellini (2004) for central stars of LMC planetary nebulae. Also, the use of Monte-Carlo simulations on the recovered parameters allows for the secure and objective determination of statistically meaningful confidence intervals around recovered parameters, indeed, the full covariance matrix

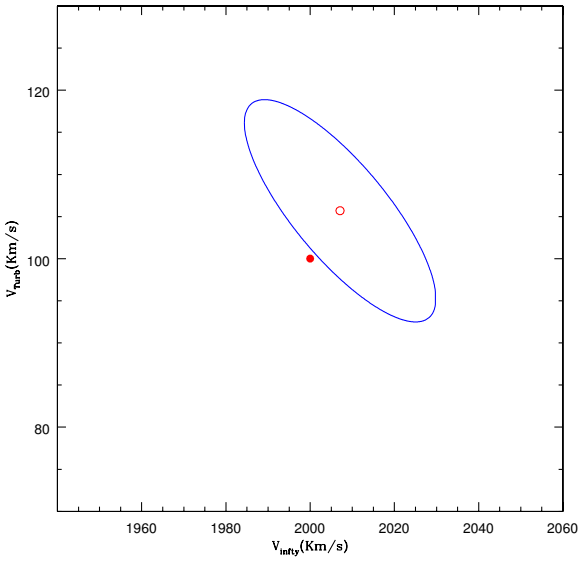

Fig. 6. Correlation between V_∞ and V_{turb} calculated for synthetic profile with S/N = 50.

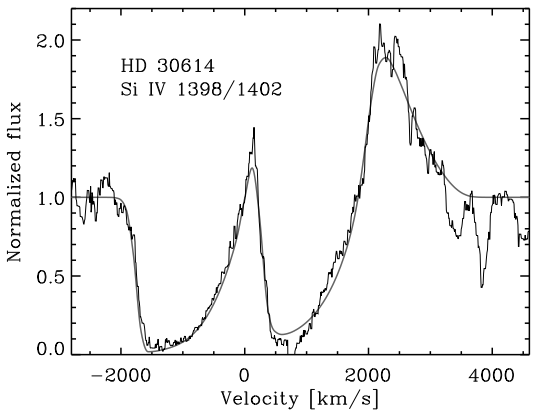

Fig. 7. Fit of the Si IV 1392/1402 Å line in HD 30614. The dotted line is the fit.

TABLE 2

PARAMETERS OF THE WIND OF HD 30814 AND HD 66811[a]

Parameter	HD 66811 C IV 1548/1550 Å		HD 30814 Si IV 1398/1402 Å	
	This work	Published	This work	Published
V_∞ (km s^{-1})	1550±16	1550±50	2137±21	2200±60
V_{turb} (km s^{-1})	240±24	190±70	287±30	290±70
β	1.13±0.1	0.7±0.1	1.18±0.1	0.7±0.1
$\log \dot{M} q_{ion} q_{ex}$ ($M_\odot$/yr)	−6.99±0.15	>−7.14	−7.27±0.15	>−8.4

[a]Determined in this work together with the same data obtained by Groenewegen & Lamers (1989).

is available. But we have to stress that the parameter obtained by this method is not the mass loss rate $\dot{M}$ itself, but rather the product $\dot{M} q_{ion} q_{ex}$. There is no easy way to separate these quantities on the base of low dispersion and low S/N data on which only few lines are measurable. Our method helps to obtain more reliable estimates of the product in an easier way, but the final decision on how to disentangle $\dot{M}$ and the ionization and excitation fractions depends on the studied object and on the problem which needs to be solved.

An important advantage of our method, compared to other fitting algorithms, is a minimal effect of the initial guess on the final solution. This is because the method does not rely on a series expansion. The genetic algorithm requires only crude margins on the parameters to find the maximum of the likelihood surface. In case the maximum is not within the proposed ranges, the population migrates to the parameter limit closest to the maximum. A subsequent run with new ranges that increase this limit usually leads to a successful solution. The price to pay is only an increased number of profile evaluations. But fast computers make this price affordable. The calculation of one generation of "bugs" takes less than 2 minutes on a Pentium IV-class computer. Usually fifty to a hundred generations are needed to fit one line profile. Each "bug" in a generation is independent of the rest of the population, so a simple parallelization increases the speed of the calculation almost proportionally to the number of available processors.

The method has, however, a few disadvantages. First of all, the choice of the weights σ_i in Eq. (9) is not automatic. The observed profiles frequently have overlapped absorption lines of other elements, interstellar lines or absorption components of the same star and the same element but which are not formed in the wind. The weights σ_i should be chosen lower in the affected bands so the likelihood is calculated

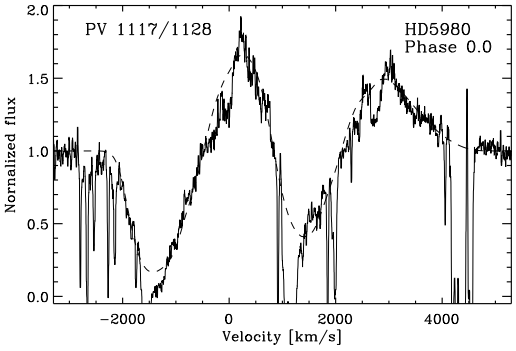

Fig. 8. Fit of the P V 1117/1129 line in the LMC star HD 5980. The thin line is the observed spectrum. The dashed line is the fit. Small weight was applied to the interstellar absorption line, which contaminates the P Cyg profile.

using only the pixels which belong to the line. Figure 8 shows the fit of the P V 1117/1128 Å line in the star HD 5980 as an example of the performance of the code on a highly contaminated line. The FUSE spectra are characterized by a huge number of interstellar absoption line. In the above case, a small weight (large errors) was assigned to the bands with high contamination. As seen from Fig. 8, the code finds a satisfactory fit which reproduces the P Cyg line profile, avoiding the contamination.

Another problem is that the parameters can be obtained only from a grid. As a result, the code never converges to the exact solution but to the node of the parameter's grid which is closest to, but not exactly at, the maximum of the likelihood surface. That might cause the systematic error seen in Fig. 4. One possible solution to this problem is a second run of the code with smaller ranges of the parameters around the solution found. Another approach is to combine a genetic algorithm with a classical minimization method. The genetic algorithm guarantees that the solution will be near the global maximum

of the likelihood surface and then the classical minimization algorithm starts from that point and finds the exact solution. Until now we have explored only the first option. The combination of the algorithms and their application to a wide range of objects, together with the problem of separating the mass loss rate from the ionization fraction, will be subject of the next paper of this series.

We thank G. Koenigsberger for many usefull discutions and for critical reading of the manuscript. This work was supported by CONACyT grants 40864 and 42809, and UNAM/DGAPA grant IN107202.

REFERENCES

Arrieta, A., & Stangellini, L. 2004, ESO Astrophysics Symposia, Planetary Nebulae beyond the Milky Way, eds. L. Stangellini, J. R. Walsh, & N. Douglas, in press

Charbonneau, P. 1995, ApJS, 101, 309

Georgiev, L. N., & Koenigsberger, G. 2004, A&A, 423, 267

Groenewegen, M. A. T., & Lamers, H. J. G. L. M. 1989, A&AS, 79, 359

Lamers, H. J. G. L. M., Cerruti-Sola, M., & Perinotto, M. 1987, ApJ, 314, 726

Lamers, H. J. G. L. M., Haser, S., de Koter, A., & Leitherer, C. 1999, ApJ, 516, 872

Metcalfe, T. S. 2003, ApJ, 587L, 43

Sevenster, M., Saha, P., Valls-Gabaud, D., & Fux, R. 1999, MNRAS, 307, 584

Sobolev, V. V. 1958, Theoretical Astrophysics, ed. V. A. Ambartsumian (Pergamon Press: New York)

Steffen, M. 1990, A&A, 239, 443

Teriaca, L., Banerjee, D., & Doyle, J. G. 1999, A&A, 349, 636

Leonid Georgiev and Xavier Hernández: Instituto de Astronomía, UNAM, Apdo. Postal 70-264, 04510 México, D. F., México (georgiev@astroscu.unam.mx; xavier@astroscu.unam.mx).